Supramolecular Chemistry

International Edition: DOI: 10.1002/anie.201901882
German Edition: DOI: 10.1002/ange.201901882

Efficient Room-Temperature Phosphorescence of a Solid-State Supramolecule Enhanced by Cucurbit[6]uril

*Zhi-Yuan Zhang, Yong Chen, and Yu Liu**

Abstract: *Efficient emission of purely organic room-temperature phosphorescence (RTP) is of great significant for potential application in optoelectronics and photobiology. Herein, we report an uncommon phosphorescent effect of organic single molecule enhanced by resulting supramolecular assembly of host–guest complexation. The chromophore bromophenyl-methyl-pyridinium (PY) with different counterions as guests display various phosphorescence quantum yields from 0.4 % to 24.1 %. Single crystal X-ray diffraction results indicate that the chromophore with iodide counterion (PYI) exhibits the highest efficiency maybe due to the halogen-bond interactions. Significantly, the nanosupramolecular assembly of PY chloride complexation with the cucurbit[6]uril gives a greatly enhanced phosphorescent quantum yield up to 81.2 % in ambient. Such great enhancement is because of the strict encapsulation of cucurbit[6]uril, which prevents the nonradiative relaxation and promotes intersystem crossing (ISC). This supramolecular assembly concept with counterions effect provides a novel approach for the improvement of RTP.*

Organic room-temperature phosphorescent (RTP) has got tremendous attention due to their extensive application in optoelectronics[1] and photobiology,[2] such as organic light-emitting diodes[3] and bioimaging.[4] So far, most of organic RTP materials are organometallic complexes. Considering their high cost and restriction in resources, the development of purely organic (metal-free) phosphorescent materials are of great concern.[5] However, phosphorescence of purely organic molecules are fairly weak owing to their inefficient spin-orbit coupling,[6] hence massive efforts have been devoted to achieving efficient RTP by developing new methods, such as special design of structure,[7] embedding into proper matrix[8] and careful crystallization.[9] Recently, a principle of using directed heavy atom effect to facilitate the efficiency of phosphorescence (phosphorescence quantum yield 55 %) has been reported by Kim and co-workers.[10] Moreover, external heavy atom effect is proven to be another effective method in fabricating efficient phosphorescent materials (phosphorescence quantum yield 36 %).[11] On the other hand, supramolecular approach have been used extensively to construct functional materials by complexing or assembly. Noncovalent interactions, such as host-guest interaction,[12] hydrogen bonding,[13] π-π stacking[14] can alter the properties of guests greatly. Recently, Huang and co-workers reported a supramolecular strategy to enhance the efficiency (phosphorescence quantum yield 24.3 %) and extend the lifetime of phosphorescence by constructing crystalline framework.[13] Moreover, it is well known that the complexation between macrocycles (especially for cyclodextrin[15] and cucurbituril[16]) and luminous guests have great impact on photoluminescent characters. More recently, Tian and co-workers reported a decent quantum yield (16.9 %) of organic RTP induced by hydrogen bonding of chromophore modified cyclodextrin.[5] Besides, cucurbituril is a good host to improve the fluorescence quantum yield through preventing aggregation[17] or forming supramolecular polymer.[18] However, effective strategy of improving the phosphorescence quantum yield of organic single molecule is still rare. Herein, we report an uncommon enhancement of phosphorescence quantum yield of bromophenyl-methyl-pyridinium chloride (PYCl) from 2.6 % to 81.2 % by complexing with cucurbit[6]uril (CB6), which should be the highest phosphorescence quantum yield of purely organic systems so far. One explanation for this great enhancement is probably macrocycle effect rather than heavy atom effect. Besides, results of single crystal X-ray diffraction indicate that halogen-bonding interactions may contribute to the high efficiency of bromophenyl-methyl-pyridinium iodide (PYI). This design method of supramolecular assembly couple with counterions effect offers a novel approach for the enhancement of RTP.

Organic salts 4-(4-bromophenyl)-*N*-methylpyridinium with different counterions (PYX, X = Cl, Br, I and PF_6) had been designed and synthesized. The 4-(4-bromophenyl)-*N*-methylpyridinium with chloridion as the counterion (PYCl) showed a blue emission peak at 426 nm with the average lifetime of 5.76 μs and quantum yields of 2.6 % (Figures 1 c and S4 c in the Supporting Information). The microsecond-scaled lifetime confirmed that the emission was phosphorescence. However, exchanging chloridion to iodide (PYI) resulted in luminous yellow emission at 575 nm with quantum yields of 24.1 % and average lifetime of 5.61 μs (Figures 1 a and S4a). This great improvement of efficiency spurred us to explore congener bromide (PYBr) and a larger hexafluorophosphate ($PYPF_6$). PYBr exhibited weaker yellow emission (peak at 470 nm) in 4.6 % efficiency, while the emission of $PYPF_6$ was very weak cyan (peak at 510 nm) with the

[*] Z.-Y. Zhang, Dr. Y. Chen, Prof. Dr. Y. Liu
College of Chemistry
State Key Laboratory of Elemento-Organic Chemistry
Nankai University
Tianjin 300071 (China)
E-mail: yuliu@nankai.edu.cn
Prof. Dr. Y. Liu
Collaborative Innovation Center of Chemical Science and Engineering (Tianjin)
Nankai University
Tianjin 300072 (China)
Supporting information and the ORCID identification number(s) for the author(s) of this article can be found under: https://doi.org/10.1002/anie.201901882.

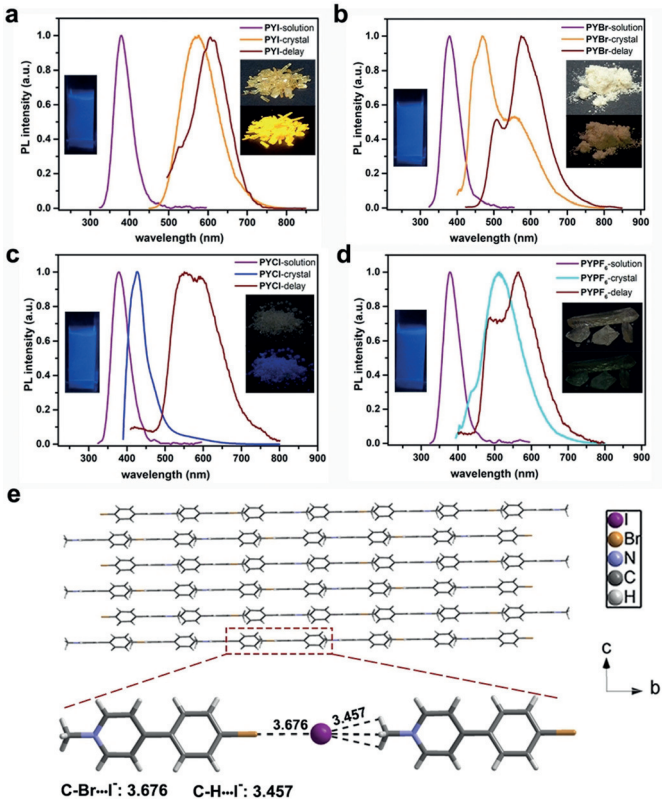

Figure 1. a) Photoluminescence spectra of PYI in solid (orange line), solution (violet line) and phosphorescence spectra (wine line); b) Photoluminescence spectra of PYBr in solid (orange line), solution (violet line) and phosphorescence spectra (wine line); c) Photoluminescence spectra of PYCl in solid (blue line), solution (violet line) and phosphorescence spectra (wine line); d) Photoluminescence spectra of $PYPF_6$ in solid (cyan line), solution (violet line) and phosphorescence spectra (wine line) (inset: left, pictures of PYX in solution under 304 nm lamp; right, PYX crystal under ambient light and 365 nm lamp); e) Single-crystal X-ray diffraction analysis of PYI.

quantum yield of 0.4% (Figure 1 and Table S1). Besides, photoluminescence spectra at 110 K and phosphorescence spectra also confirmed their phosphorescent property (Figures 1 and S5). Different photophysical properties of PYX hinted the critical role of counterions in the solid state. The same absorbance peak at 304 nm and emission peak at 380 nm in solution indicated that the counterions no longer exerted influence on cation moiety in solution, which proved the aforementioned inference (Figure S2).

The intense emission of PYI focused us to explore the origin. The crystals of PYI, PYBr, PYCl, and $PYPF_6$ were grown by evaporating solvent slowly in ambient (Figure S6). Phase purity was confirmed by XRD (Figure S7). Torsion angle and π-π stacking are inspected firstly as they are two crucial factors for the photophysical properties of chromophore. PYI and $PYPF_6$ possessed similar torsion angle (35.41° and 32.23°), but showed very different quantum yields (Figure S6a, j). Besides, smaller torsion angle (10.85° for PYBr and 4.08° for PYCl) were not beneficial to the improvement of efficiency (Figure S6d,g). Therefore, torsion angle is turned out to be not the vital factor for the high efficiency. Moreover, the π-π distances between adjacent molecules were larger for PYBr (3.716, 3.636 Å) and smaller for PYCl (3.392, 3.439 Å) and $PYPF_6$ (3.421 Å) than that of PYI (3.581, 3.506 Å), which negated the other reason of efficient phosphorescence (Figures S6b,e,h,k). After investigating the packing mode, we found that PYI stacked head-to-tail to form linear structure connecting by halogen bonds in the angle of 180° (Figure 1e). It was reported that the halogen bond between aryl halide and halide ion would result in a partial delocalization of the electrons from halide ion to the bromine of the aryl halide. We proposed that the C–Br···I^- halogen bond in PYI led to the electron delocalization of I^-, which promoted the spin-orbit coupling as well as the subsequent triplet generation and thus resulted in the high RTP efficiency.[19] In addition, the halogen bonds accompanying with multiple hydrogen bonds locked molecules in different directions, probably restricting the molecular motion and reducing the non-radiative decay (Figure S6c). While there were also tremendous hydrogen bonds for PYBr, PYCl, and $PYPF_6$ to limit the molecular vibration in crystal, no efficient phosphorescence was observed which further verified the paramount importance of halogen bonds for efficient emission. When dissolving PYI in water, the halogen bond and the hydrogen bond were destroyed which made the generation of triplet not efficiently enough and the loss of triplet to vibration increased. Therefore, PYI exhibited fluorescent emission in solution.

This great enhancement of emission manipulated by counterions inspired us to improve the efficiency by other method. The phosphor should exhibit more intensive photoluminescence in a more restricted circumstance, such as supramolecular macrocyclic host. It was reported that CB[6] could only slide over viologen units but not engulf.[20] This interesting behavior gives us an anticipation that CB[6] is able to offer a restricted condition for PYCl to promote the phosphorescence by forming complexes. The poor solubility of CB[6] ($< 10^{-5}$ M) tremendously limited the basic characterization in solution and spurred us to explore operable approach to prepare the complex.[21] Grinding was a good candidate because of its high efficiency and convenience in synthesizing complexes in the solid state.[22] 1 mmol CB[6] and 1 mmol PYCl was ground in agate mortar. After grinding for 3 minutes, partial green luminance appeared in the blue powder under 365 nm lamp (Figure S8g). That hinted some interactions between PYCl and CB[6]. To further mixing, a drop of deionized water was added and further grinding. Surprisingly, intense and uniform green emission occurred (Figure S8h,i). After drying in vacuum, the green emission reserved (Figure S8j). Emission spectra displayed two peaks of 388 and 500 nm (Figure 2a). Excitation spectra indicated that 338 and 360 nm contributed to the emissions of 388 nm and 500 nm, respectively (Figure S9a). The time-resolved photoluminescence decay curves confirmed that the emission of 388 nm was fluorescence with a short lifetime of 3.62 ns and the emission of 500 nm was phosphorescence with a long lifetime of 5.40 ms, more than 930-folds prolonged comparing to PYCl (Figures 2b and S9d,e). The steady-state phosphorescence spectra also verified its phosphorescence properties (Figure 2a). Blank experiments showed that CB[6] had no absorbance and emission, which further confirmed that the

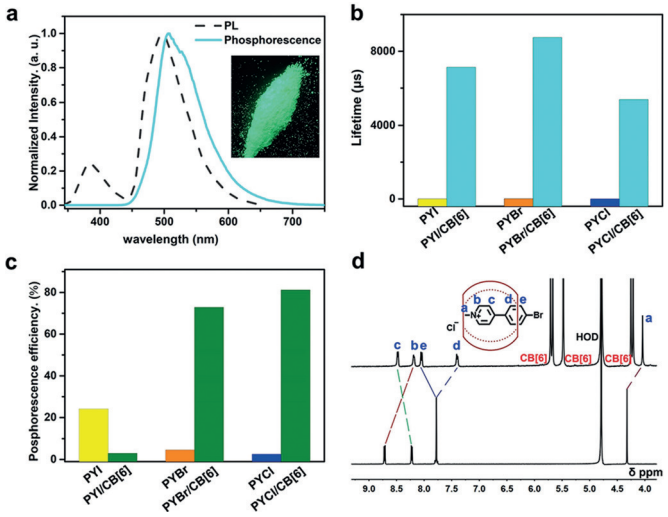

Figure 2. Photophysical properties of PYCl and PYCl/CB[6] in solid under ambient conditions. a) Steady-state photoluminescence (PL, gray dashed line) and phosphorescence (cyan solid line) spectra of PYCl/CB[6] complex under 334 nm excitation (inset: photograph of PYCl/CB[6] under 365 nm); b) Lifetime of PYX and PYX/CB[6]; c) Phosphorescence quantum efficiency of PYX and PYX/CB[6]; d) ^{1}H NMR spectra of PYCl/CB[6] and PYCl.

phosphorescence came from PYCl in the PYCl/CB[6] complex (Figure S9b,c). In general, strong green emission mean high phosphorescence quantum efficiency. Indeed, absolute phosphorescence quantum efficiency (Φ) of the complex was as high as 81.2% (Figures 2c and S25). To the best of our knowledge, it is the highest Φ among purely organic RTP materials (Figure S1). The similar photoluminescence spectra of 10% and 100% PYCl at PYCl/CB[6] indicated little influence of molar ratio on the phosphorescence in this range (Figure S10a). The 60% increasing of phosphorescent intensity after drying indicated that water was unfavorable for the phosphorescence, which fitted well with the literature (Figure S10b).[23] Moreover, the relative intensity of phosphorescence increased at low temperature, indicating the additional suppression of molecular motions by cryogenic temperature (Figure S12). To investigate the influence of counterions, we prepared the PYBr/CB[6] and PYI/CB[6] complex in same method. Both of them exhibited similar photoluminescence spectra and lifetime (Figures 2b and S11). The phosphorescence quantum yield was 72.9% for PYBr/CB[6], but only 3.0% for PYI/CB[6] (Figure 2c). This unusually low efficiency of PYI/CB[6] made us consider the influence of iodide counterion. As pyridinium iodides can form charge transfer complex which will quench photoluminescence, we proposed that this maybe the cause of low efficiency for PYI/CB[6].[24] Brownish yellow color of PYI/CB[6] solid hinted the existence of charge transfer complex, very different from the pure white of PYBr/CB[6] and PYCl/CB[6] (Figure S13). Furthermore, the charge-transfer absorption band of 350–400 nm for PYI has also appeared for PYI/CB[6] complex in the solid state in UV/Vis spectra (Figure S13). In PYI/CB[6], the weak halogen-bond interactions may also existed and benefit the RTP to some extent, but the formation of the strong charge transfer complex between PY^+ cation and I^- counterion would greatly quench the PL. As a joint result, PYI/CB[6] exhibited a fairly low quantum yield.

The sharp promotion of phosphorescent properties of PYCl/CB[6] motivated us to explore the origin. As basic principles, the improvement of phosphorescence quantum efficiency and extension of lifetime mainly depended on enhancing of ISC and suppressing of nonradiative relaxation.[6] On the foundation of obtained and reported results,[25] we proposed a rational mechanism for this enhancement. The photoluminescence of PYCl/CB[6] would be influenced by two noncovalent interactions: i) Host-guest interaction between CB[6] and PYCl by complexing; ii) External interactions (such as hydrogen bonding) between the portal carbonyl moiety of CB[6] and the pyridine ring hydrogen atoms of PYCl. The first step was to identify the host–guest interaction. PYCl/CB[6] complex had a better solubility in water than CB[6], but remained fairly low ($< 10^{-4}$ M). ^{1}H NMR revealed that methyl protons H_a and the aromatic protons H_b, and H_d of PYCl underwent enormous upfield shifts of 0.31, 0.54 and 0.35 ppm, respectively (Figure 2d). This complexation-induced shifts indicated that PYCl was deeply encapsulated in the CB[6] cavity. The COSY ^{1}NMR assigned the protons and further verified the complexion (Figures S14,S15). MALDI-TOF MS also proved the formation of PYCl/CB[6] complex (Figure S16). Furthermore, if the phosphorescence of PYCl/CB[6] was originated from the external interaction between portal carbonyl moiety of CB[6] and the pyridine ring hydrogen atoms of PYCl, the replacing of CB[6] to smaller homolog CB[5] should have little effect on the phosphorescence. However, PYCl/CB[5] had a weak blue-purple emission peak at 420 nm with fairly low efficiency (3.2%) and short lifetime (8.52 μs), quite different from that of PYCl/CB[6] (Figures S17a,b, S20d,i and Table S1). Besides, the smaller cavity (4.4 Å) of CB[5] made it impossible to bond with PYCl (6.3 Å) which was confirmed by the unvaried chemical shift (Figure S18).[21,26] Therefore, we concluded that the host–guest interaction between CB[6] and PYCl, but not external interaction, was responsible for the promotion of phosphorescent properties. Moreover, we replaced host CB[6] with larger homolog CB[7] to identify the size effect on the boosting for phosphorescence. The 7.3 Å diameter of CB[7] was enough to bond PYCl which was supported by the large chemical shift of PYCl (Figure S19).[27] PYCl/CB[7] had a weak phosphorescent emission peak at 482 nm with a long lifetime of 2.20 ms in solid (Figures S17c,d, S20e,j and Table S1). But the 3.3% of efficiency was far below the 81.2% of PYCl/CB[6] (Table S1). This result demonstrated that the phosphorescent properties were tightly dependent on the size of host and CB[6] was the best candidate for the facilitation of phosphorescence. We further investigated the photoluminescent properties of PYCl/CB[6] in aqueous solution at various concentration (Figure S21). Only fluorescence (378 nm) was observed, indicating that the phosphorescence of PYCl/CB[6] only existed in the solid state. We deduced that the collision of H_2O to PYCl would deactivate the triplet states and therefore quench phosphorescence in aqueous solution.

Interestingly, the PYCl/CB[6] possessed fibrous structure with varying lengths and widths of several micrometers which

were revealed by transmission electron microscopy (TEM) (Figure 3a). Benefiting from the photoluminescent property of PYCl/CB[6], we further confirmed the nanofiber by laser scanning confocal microscope (LSCM). Luminous fibers were

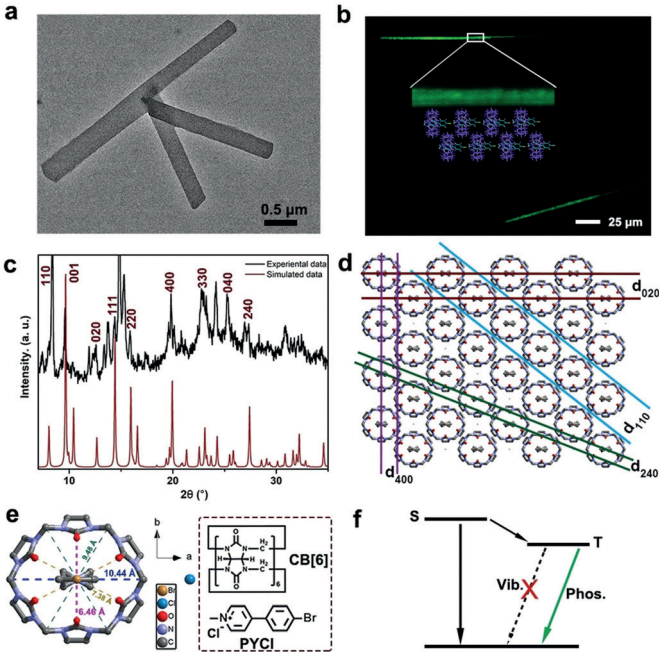

Figure 3. a) TEM image of PYCl/CB[6]; b) LSCM image of PYCl/CB[6] (inset: the cartoon of linear array); c) XRD patterns of PYCl/CB[6] (black line: experimental data; red line: simulated data based on crystal); d) Schematic illustration of planes based on XRD; e) Crystal structure of PYCl/CB[6] view in c-axis and their chemical structure; f) The efficient phosphorescence emission of PYCl/CB[6].

observed, reaching the length of 170 μm and width of 3 μm (Figures 3b and S22). It's well known that cucurbit[*n*]urils complexes (especially CB[6] complexes) tend to possess a close-packed arrangement with infinite guest-filled channels in solid.[28] Therefore, we proposed that the nanofibers was probably in possession of a similar array. That was, PYCl/CB[6] complexes stacked tightly in the same direction which was verified by powder X-ray diffraction (XRD) pattern (Figure 3c,d). The XRD peaks with d-spacings of 10.61, 5.56, and 3.68 Å were indexed, respectively, as diffractions from the (110), (220), and (330) planes. The d-spacings of 7.02, 4.47, 3.53, and 3.26 Å were assigned to (020), (400), (040), and (240) planes (Figure 3c,d). All of them were consistent with the calculated data based on crystal (Table S4 and Figure S23).

To obtain more direct evidence for the complex, single crystal was grown. We kept the aqueous solution of PYCl/CB[6] at room temperature for solvent evaporation. Several weeks later, clear needle-like crystal appeared and was characterized by X-ray diffraction. Unfortunately, better crystal data were unavailable after months of trying and the disorder of the PYCl in crystal made it hard to identify its configuration, but there were still valuable information about the complex (Figure S23). The skeleton of CB[6] possessed an ellipsoidal deformation with the major and minor axis of 10.44 Å and 6.46 Å, extended 0.65 Å and shortened 0.49 Å respectively compared with that of CB[6] without guest (Figures 3e and S23a,b).[28b] This great deformation of CB[6] and reports about cucurbiturils increasing intersystem crossing[16c,d] uncovered the origin of uncommon promotion of phosphorescence properties in solid: The tightly enclosing of CB[6] suppressed the vibrational relaxation of PYCl immensely and the short distance between PYCl and carbonyl group in CB[6] boosted the ISC, resulting the great improvement of phosphorescent efficiency and lifetime (Figure 3f). Moreover, the macrocycle possibly contributed to this promotion by shielding quenchers and preventing potential self-quenching of chromophores. However, the as-confirmed low quantum efficiency of CB[7]/PYCl revealed that these functions were negligible because CB[7] could also provide such functions.

In conclusion, a novel fibrous supramolecular assembly has been constructed by chromophore PYCl and CB[6] which shows up to 81.2% phosphorescence quantum yield. Interestingly, PY with different counterions exhibits various quantum efficiency from 0.4% to 24.1%. Notably, the complexion of CB[6] sharply promotes phosphorescence quantum efficiency. Such great improvement is attribute to the tightly encapsulation of CB[6] which suppresses the non-radiative decay and promotes the ISC. Moreover, the significant enhancement for phosphorescence is particular for CB[6], larger or smaller host display no such facilitation. This supramolecular assembly principle provides a convenient method for the promotion of RTP.

Acknowledgements

This work was supported by NSFC (21432004, 21861132001, 21672113, 21772099).

Conflict of interest

The authors declare no conflict of interest.

Keywords: counterion effect · cucurbit[6]uril · high phosphorescent efficiency · host–guest complex · supramolecular chemistry

How to cite: *Angew. Chem. Int. Ed.* **2019**, *58*, 6028–6032
Angew. Chem. **2019**, *131*, 6089–6093

[1] H. Xu, R. Chen, Q. Sun, W. Lai, Q. Su, W. Huang, X. Liu, *Chem. Soc. Rev.* **2014**, *43*, 3259–3302.
[2] Q. Zhao, C. Huang, F. Li, *Chem. Soc. Rev.* **2011**, *40*, 2508–2524.
[3] a) Q. Zhang, B. Li, S. Huang, H. Nomura, H. Tanaka, C. Adachi, *Nat. Photonics* **2014**, *8*, 326; b) R. Kabe, N. Notsuka, K. Yoshida, C. Adachi, *Adv. Mater.* **2016**, *28*, 655–660.
[4] a) G. Zhang, G. M. Palmer, M. W. Dewhirst, C. L. Fraser, *Nat. Mater.* **2009**, *8*, 747; b) X. Zhen, C. Xie, K. Pu, *Angew. Chem. Int. Ed.* **2018**, *57*, 3938–3942; *Angew. Chem.* **2018**, *130*, 4002–4006.
[5] a) D. Li, F. Lu, J. Wang, W. Hu, X.-M. Cao, X. Ma, H. Tian, *J. Am. Chem. Soc.* **2018**, *140*, 1916–1923; b) Q. Li, Y. Tang, W. Hu, Z. Li, *Small* **2018**, *14*, 1801560.

[6] M. Baroncini, G. Bergamini, P. Ceroni, *Chem. Commun.* **2017**, *53*, 2081 – 2093.
[7] a) Z. He, W. Zhao, J. W. Y. Lam, Q. Peng, H. Ma, G. Liang, Z. Shuai, B. Z. Tang, *Nat. Commun.* **2017**, *8*, 416; b) Z. Yang, Z. Mao, X. Zhang, D. Ou, Y. Mu, Y. Zhang, C. Zhao, S. Liu, Z. Chi, J. Xu, Y.-C. Wu, P.-Y. Lu, A. Lien, M. R. Bryce, *Angew. Chem. Int. Ed.* **2016**, *55*, 2181 – 2185; *Angew. Chem.* **2016**, *128*, 2221 – 2225.
[8] a) N. Gan, H. Shi, Z. An, W. Huang, *Adv. Funct. Mater.* **2018**, *28*, 1802657; b) S. Kuila, K. V. Rao, S. Garain, P. K. Samanta, S. Das, S. K. Pati, M. Eswaramoorthy, S. J. George, *Angew. Chem. Int. Ed.* **2018**, *57*, 17115 – 17119; *Angew. Chem.* **2018**, *130*, 17361 – 17365.
[9] a) J. Wei, B. Liang, R. Duan, Z. Cheng, C. Li, T. Zhou, Y. Yi, Y. Wang, *Angew. Chem. Int. Ed.* **2016**, *55*, 15589 – 15593; *Angew. Chem.* **2016**, *128*, 15818 – 15822; b) C.-R. Wang, Y.-Y. Gong, W.-Z. Yuan, Y.-M. Zhang, *Chin. Chem. Lett.* **2016**, *27*, 1184 – 1192; c) A. Forni, E. Lucenti, C. Botta, E. Cariati, *J. Mater. Chem. C* **2018**, *6*, 4603 – 4626; d) J. Yang, X. Zhen, B. Wang, X. Gao, Z. Ren, J. Wang, Y. Xie, J. Li, Q. Peng, K. Pu, Z. Li, *Nat. Commun.* **2018**, *9*, 840.
[10] O. Bolton, K. Lee, H.-J. Kim, K. Y. Lin, J. Kim, *Nat. Chem.* **2011**, *3*, 205.
[11] J. Wang, X. Gu, H. Ma, Q. Peng, X. Huang, X. Zheng, S. H. P. Sung, G. Shan, J. W. Y. Lam, Z. Shuai, B. Z. Tang, *Nat. Commun.* **2018**, *9*, 2963.
[12] X.-L. Ni, S. Chen, Y. Yang, Z. Tao, *J. Am. Chem. Soc.* **2016**, *138*, 6177 – 6183.
[13] L. Bian, H. Shi, X. Wang, K. Ling, H. Ma, M. Li, Z. Cheng, C. Ma, S. Cai, Q. Wu, N. Gan, X. Xu, Z. An, W. Huang, *J. Am. Chem. Soc.* **2018**, *140*, 10734 – 10739.
[14] E. Lucenti, A. Forni, C. Botta, L. Carlucci, C. Giannini, D. Marinotto, A. Previtali, S. Righetto, E. Cariati, *J. Phys. Chem. Lett.* **2017**, *8*, 1894 – 1898.
[15] a) I. Lammers, J. Buijs, G. van der Zwan, F. Ariese, C. Gooijer, *Anal. Chem.* **2009**, *81*, 6226 – 6233; b) A. Muñoz de la Peña, M. Mahedero, C. A. Bautista Sánchez, *Analusis* **2000**, *28*, 670 – 678.
[16] a) S.-H. Li, X. Xu, Y. Zhou, Q. Zhao, Y. Liu, *Org. Lett.* **2017**, *19*, 6650 – 6653; b) Y. Xia, S. Chen, X.-L. Ni, *ACS Appl. Mater. Interfaces* **2018**, *10*, 13048 – 13052; c) P. Montes-Navajas, L. Teruel, A. Corma, H. Garcia, *Chem. Eur. J.* **2008**, *14*, 1762 – 1768; d) P. Montes-Navajas, H. Garcia, *J. Phys. Chem. C* **2010**, *114*, 2034 – 2038.
[17] F. Biedermann, E. Elmalem, I. Ghosh, W. M. Nau, O. A. Scherman, *Angew. Chem. Int. Ed.* **2012**, *51*, 7739 – 7743; *Angew. Chem.* **2012**, *124*, 7859 – 7863.
[18] H.-J. Kim, D. R. Whang, J. Gierschner, S. Y. Park, *Angew. Chem. Int. Ed.* **2016**, *55*, 15915 – 15919; *Angew. Chem.* **2016**, *128*, 16147 – 16151.
[19] G. Cavallo, P. Metrangolo, R. Milani, T. Pilati, A. Priimagi, G. Resnati, G. Terraneo, *Chem. Rev.* **2016**, *116*, 2478 – 2601.
[20] S. Choi, J. W. Lee, Y. H. Ko, K. Kim, *Macromolecules* **2002**, *35*, 3526 – 3531.
[21] J. W. Lee, S. Samal, N. Selvapalam, H.-J. Kim, K. Kim, *Acc. Chem. Res.* **2003**, *36*, 621 – 630.
[22] A. L. Garay, A. Pichon, S. L. James, *Chem. Soc. Rev.* **2007**, *36*, 846 – 855.
[23] S. Xu, R. Chen, C. Zheng, W. Huang, *Adv. Mater.* **2016**, *28*, 9920 – 9940.
[24] a) E. M. Kosower, J. A. Skorcz, W. M. Schwarz, J. W. Patton, *J. Am. Chem. Soc.* **1960**, *82*, 2188 – 2191; b) G. Saielli, *J. Phys. Chem. A* **2008**, *112*, 7987 – 7995.
[25] T.-H. Meng, Y. Zhou, Z.-Z. Gao, Q.-Y. Liu, Z. Tao, X. Xiao, *J. Inclusion Phenom. Macrocyclic Chem.* **2018**, *90*, 357 – 363.
[26] J. Kim, I.-S. Jung, S.-Y. Kim, E. Lee, J.-K. Kang, S. Sakamoto, K. Yamaguchi, K. Kim, *J. Am. Chem. Soc.* **2000**, *122*, 540 – 541.
[27] G. A. Vincil, A. R. Urbach, *Supramol. Chem.* **2008**, *20*, 681 – 687.
[28] a) S. Liu, C. Ruspic, P. Mukhopadhyay, S. Chakrabarti, P. Y. Zavalij, L. Isaacs, *J. Am. Chem. Soc.* **2005**, *127*, 15959 – 15967; b) D. Bardelang, K. A. Udachin, D. M. Leek, J. A. Ripmeester, *CrystEngComm* **2007**, *9*, 973 – 975.

Manuscript received: February 12, 2019
Revised manuscript received: March 5, 2019
Accepted manuscript online: March 7, 2019
Version of record online: March 26, 2019

